AMERICAN SOCIETY FOR MICROBIOLOGY | mBio®

RESEARCH ARTICLE

Quorum Sensing Coordinates Cooperative Expression of Pyruvate Metabolism Genes To Maintain a Sustainable Environment for Population Stability

Lisa A. Hawver,[a] Jennifer M. Giulietti,[a] James D. Baleja,[b] Wai-Leung Ng[a,c]

Department of Molecular Biology and Microbiology, Tufts University School of Medicine, Boston, Massachusetts, USA[a]; Department of Developmental, Molecular and Chemical Biology, Tufts University School of Medicine, Boston, Massachusetts, USA[b]; Program in Molecular Microbiology, Sackler School of Graduate Biomedical Sciences, Tufts University, Boston, Massachusetts, USA[c]

ABSTRACT **Quorum sensing (QS) is a microbial cell-cell communication system that regulates gene expression in response to population density to coordinate collective behaviors. Yet, the role of QS in resolving the stresses caused by the accumulation of toxic metabolic by-products at high cell density is not well defined. In response to cell density, QS could be involved in reprogramming of the metabolic network to maintain population stability. Using unbiased metabolomics, we discovered that *Vibrio cholerae* mutants genetically locked in a low cell density (LCD) QS state are unable to alter the pyruvate flux to convert fermentable carbon sources into neutral acetoin and 2,3-butanediol molecules to offset organic acid production. As a consequence, LCD-locked QS mutants rapidly lose viability when grown with fermentable carbon sources. This key metabolic switch relies on the QS-regulated small RNAs Qrr1-4 but is independent of known QS regulators AphA and HapR. Qrr1-4 dictate pyruvate flux by translational repression of the enzyme AlsS, which carries out the first step in acetoin and 2,3-butanediol biosynthesis. Consistent with the idea that QS facilitates the expression of a common trait in the population, AlsS needs to be expressed cooperatively in a group of cells. Heterogeneous populations with high percentages of cells not expressing AlsS are unstable. All of the cells, regardless of their respective QS states, succumb to stresses caused by toxic by-product accumulation. Our results indicate that the ability of the bacteria to cooperatively control metabolic flux through QS is critical in maintaining a sustainable environment and overall population stability.**

IMPORTANCE **Our work reveals a novel role for *Vibrio cholerae* quorum sensing (QS) in relieving the stresses caused by toxic metabolite accumulation when the population becomes crowded through metabolic reprogramming. QS enables *V. cholerae* switching from a low cell density energy-generating metabolism that is beneficial to individuals at the expense of the environment to a high cell density mode that preserves environmental habitability by sacrificing individual fitness. This cooperative switch provides a stable environment as the common good in maintaining the stability of the community. However, the common good can be exploited by uncooperative mutants that pollute the environment, causing population collapse. Our findings provide insights into the metabolic stress response of a major human pathogen, with implications for our understanding of microbial social biology and cooperation from an ecological and evolutionary perspective.**

Received 6 October 2016 **Accepted** 8 November 2016 **Published** 6 December 2016

Citation Hawver LA, Giulietti JM, Baleja JD, Ng W-L. 2016. Quorum sensing coordinates cooperative expression of pyruvate metabolism genes to maintain a sustainable environment for population stability. mBio 7(6):e01863-16. doi:10.1128/mBio.01863-16.

Editor Bonnie Bassler, Princeton University

Copyright © 2016 Hawver et al. This is an open-access article distributed under the terms of the Creative Commons Attribution 4.0 International license.

Address correspondence to Wai-Leung Ng, wai-leung.ng@tufts.edu.

Many microbial collective processes are ineffective if performed by a single bacterial cell acting alone. To successfully execute these tasks, bacteria employ a cell-to-cell communication process called quorum sensing (QS), in which they produce and detect extracellular signaling molecules called autoinducers to monitor cell population density, to coordinate gene expression within a group, and to act in unison (1–4). Moreover, increasing evidence indicates that QS is linked to regulation of metabolic homeostasis and readjustment (reviewed in reference 5). Since QS is employed to monitor cell density, it is possible that QS-dependent metabolic reprogramming is used to cope with the stress caused by toxic by-product accumulation due to overpopulation. Yet, the role of metabolic reprogramming in the stability of a QS bacterial population and the link between metabolism and the social behavior of a microbial community are not clear.

Vibrio cholerae, the causative agent of the disease cholera, uses QS to control a variety of group behaviors, including virulence factor production, biofilm formation, type VI secretion, and natural competence development (6–15). The QS response of *V. cholerae* is controlled by a small-RNA (sRNA)-based regulatory system (8, 16–19). At low cell density (LCD), when extracellular autoinducer levels are low, the key QS regulator LuxO is activated by phosphorylation through the action of four parallel signaling pathways (11, 15, 20). Consequently, phosphorylated LuxO (LuxO~P) activates the transcription of the genes encoding four regulatory sRNAs called Qrr1-4 (18). Qrr1-4 function redundantly to activate the translation of the AphA regulator and inhibit

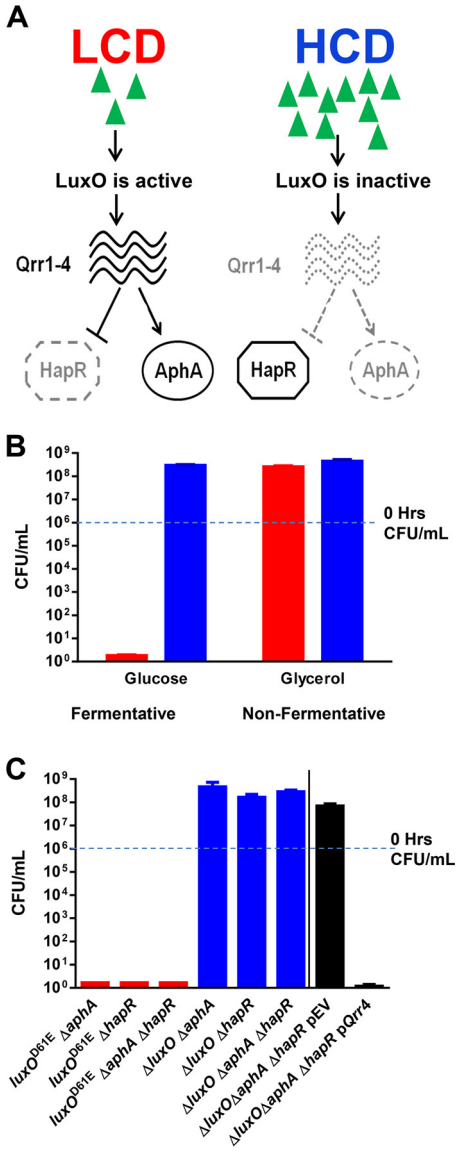

FIG 1 The roles of QS in resolving fermentative stress in *V. cholerae*. (A) Simplified view of the *V. cholerae* QS circuit. (B) Viability of *luxO*^{D61E} Δ*vpsL* (red bars) and Δ*luxO* Δ*vpsL* (blue bars) mutant cells at 72 h of growth under fermentative and nonfermentative conditions. (C) Viability of *luxO*^{D61E} (red bars) and Δ*luxO* (blue bars) mutants with additional QS mutations and the Δ*luxO* Δ*aphA* Δ*hapR* mutant strain carrying an empty plasmid or a plasmid overexpressing Qrr4 (black bar) at 72 h of growth under fermentative conditions. All strains are Δ*vpsL* mutants. The limit of detection at 72 h is 2 cells/ml of culture. The values shown are averages of at least three replicates. Error bars denote the SEM.

the translation of the HapR regulator (18–22) (Fig. 1A). At high cell density (HCD), when autoinducer levels are high, LuxO is dephosphorylated and becomes inactive. Thus, transcription of the genes for Qrr1-4 terminates and, hence, HapR is produced but AphA is not (Fig. 1A). Reciprocal production of these two regulators is believed to be crucial for the global control of QS behaviors in *V. cholerae* (21). Furthermore, Qrr sRNAs also directly control the expression of a number of targets, including feedback regulation of LuxO, a diguanylate cyclase (VCA0939), and components of a type VI secretion apparatus (17, 23–25). Yet, our understanding of the role of QS in *V. cholerae* biology is incomplete. The *V. cholerae* QS regulon is estimated to include over 100 genes (11, 21, 26, 27), significantly exceeding the number of genes related to the aforementioned processes. Thus, the QS regulon could have a broader impact on *V. cholerae* survival and fitness inside and/or outside the host.

Here we report that conversion of the central carbon metabolite pyruvate into different fermentative end products (organic acid, acetoin/2,3-butanediol [2,3-BD]) is dictated by the Qrr1-4 sRNAs in *V. cholerae*. Moreover, we provide evidence that organic acid production and acetoin/2,3-BD production are two contrasting social behaviors. The former pathway increases individual fitness by exploiting a common inhabitable environment, while the latter pathway benefits the group by sacrificing individual fitness. Massive invasion of an otherwise cooperative population by uncooperative cells that make organic acids constitutively leads to pollution of the otherwise habitable environment and kills the entire population. Our results indicate that the ability of bacteria to cooperatively control metabolic flux through QS is critical in maintaining a sustainable environment and overall population stability.

RESULTS

LCD QS mutants are sensitive to sugar fermentative stress. To begin to learn more about the physiological roles of *V. cholerae* QS, we tested if growth is adversely affected in mutants genetically locked in the LCD or HCD QS state. Here we define the *luxO*^{D61E} mutant as the LCD-locked strain since this *luxO* allele renders LuxO constitutively active by mimicking the active form of the regulator, resulting in constant production of Qrr1-4 sRNAs (Fig. 1A) (15, 17, 18). In contrast, we used the Δ*luxO* mutant as the HCD-locked strain since no Qrr1-4 sRNA is produced in the absence of LuxO (Fig. 1A) (15, 17, 18). Since carbon utilization influences many aspects of the *V. cholerae* life cycle (28–38), we first monitored the growth of these two QS mutants in M9 medium supplemented with amino acids and different carbon sources and monitored viable cell counts for at least 72 h. When no fermentable carbon source was present (e.g., medium with glycerol), the viable cell counts of both QS-locked mutants increased comparably and they maintained viability (Fig. 1B; see Fig. S1A in the supplemental material). However, when a fermentable sugar (e.g., glucose or *N*-acetylglucosamine [GlcNAc]) was present, the viable cell counts of both mutants increased during the first 24 h and the HCD-locked mutant maintained viability thereafter but the LCD-locked mutant lost viability rapidly over the next 48 h (Fig. 1B; see Fig. S1B and C). We introduced a Δ*vpsL* mutation (39–41) into our strains to rule out the potential contribution of biofilm formation. There was no difference between the observed growth phenotypes of these *vpsL* mutant strains and their *vpsL*$^+$ counterparts (see Fig. S1). *V. cholerae* strains carrying the wild-type (WT) *luxO* allele, similar to the HCD-locked mutant, were able to grow and maintain viability under these conditions (see Fig. S2 in the supplemental material). The difference in growth between these two QS mutants under this specific condition suggests that one or more metabolic pathways involved in carbon catabolism are controlled by QS and misregulated in the LCD-locked QS mutant.

Sugar fermentative stress is mediated by Qrr sRNAs independently of other QS regulators. The LCD QS regulator AphA has been shown to repress the transcription of the *alsDSO* operon involved in acetoin biosynthesis (42). Mutants unable to synthe-

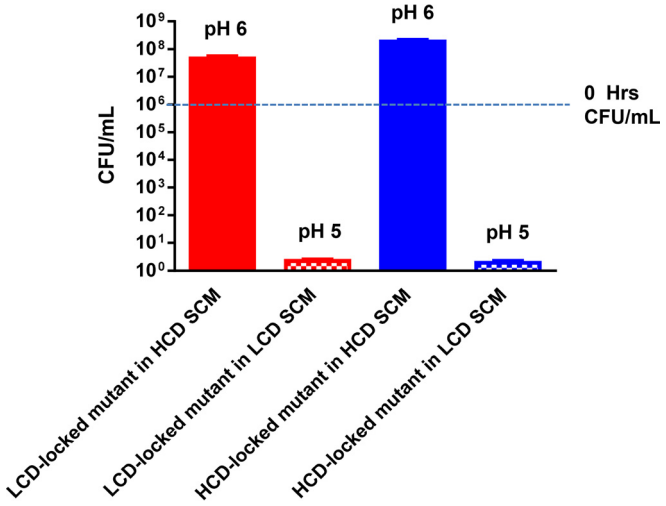

FIG 2 The LCD supernatant is toxic. The LCD-locked mutant (*luxO*^{D61E} Δ*aphA* Δ*hapR* Δ*vpsL*) (red) and the HCD-locked mutant (Δ*luxO* Δ*aphA* Δ*hapR* Δ*vpsL*) (blue) were measured at 72 h of growth in HCD SCM (solid bars) or LCD SCM (checkered bars). The blue dotted line indicates the initial cell viability of each strain at 0 h. The limit of detection at 72 h is 2 cells/ml of culture. The values shown are averages of at least three replicates. Error bars denote the SEM.

size acetoin are sensitive to glucose fermentation (42–44). Thus, the loss of viability could be attributed to constitutive production of AphA by the LCD-locked mutants, resulting in constant repression of the *alsDSO* operon. When we deleted the *aphA* gene from the LCD-locked mutant, however, the sensitivity to fermentative stress was maintained (Fig. 1C; see Fig. S3 in the supplemental material). Since HapR represses AphA expression, we predicted that a *hapR* deletion might diminish the resistance of the HCD-locked mutant to fermentative stress. However, an HCD-locked mutant lacking HapR remained resistant to fermentative stress. Similarly, LCD-locked mutants missing both AphA and HapR were still sensitive, while HCD-locked mutants missing both AphA and HapR remained resistant to fermentative stress (Fig. 1C; see Fig. S3). When Qrr4 was overexpressed ectopically in a Δ*luxO* Δ*aphA* Δ*hapR* triple mutant, these cells became sensitive to fermentative stress (Fig. 1C). These results indicate that the sensitivity to fermentative stress observed in the LCD-locked QS mutants is Qrr1-4 mediated and independent of the two QS regulators AphA and HapR. None of the *V. cholerae* Qrr1-4-regulated genes is known to be involved in resolving fermentative stress (24, 25). Our results suggest that a new physiological role for Qrr1-4 exists outside their known roles in QS gene regulation.

Cell death in LCD-locked mutants is caused by unregulated excretion of organic acids. To test if the LCD-locked mutants accumulate toxic intermediates intracellularly during glucose fermentation or if the toxicity is due to changes in the external milieu, we harvested spent culture medium (SCM) from LCD-locked mutants grown in the presence of glucose and tested if LCD SCM is toxic to the two QS-locked mutants. We found that both strains failed to maintain viability in LCD SCM (Fig. 2, checkered bars; see Fig. S4 in the supplemental material), suggesting that the SCM contains one or more toxic substances excreted by the LCD-locked mutant. It also indicates that the HCD-locked mutant does not have a mechanism to detoxify these substances. In contrast, both strains grew and maintained viability over time in SCM prepared from the HCD-locked mutant (Fig. 2, solid bars; see Fig. S4), suggesting that HCD-locked mutants produce none or low levels of these toxic by-products. After 72 h of growth, the pH of LCD SCM was ~5, whereas that of HCD SCM was ~6 (Fig. 2), consistent with the hypothesis that the toxicity is due to acidification of the external milieu during sugar fermentation by the LCD-locked mutants. In *V. cholerae*, glucose fermentation leads to several end products, some of which are acidic (Fig. 3A). Glucose is catabolized to pyruvate through glycolysis. During fermentation, pyruvate is in flux among several pathways. First, pyruvate can be fed to three different organic acid production pathways, leading to excretion of lactate, acetate, and formate (Fig. 3A). The lactate pathway provides a mechanism of NAD^+ regeneration, while ATP is generated through the acetate pathway. Pyruvate can also be converted to the neutral molecules acetoin and 2,3-BD with regeneration of NAD^+ and liberation of CO_2 (Fig. 3A). Although this pathway does not neutralize organic acids, it directs the flux of pyruvate away from organic acid production while still allowing NAD^+ regeneration, albeit without ATP production. Since the pH of LCD-locked SCM is acidic, we reasoned that the LCD-locked mutant is producing more extracellular organic acids than the HCD-locked mutant. First, we focused on SCM from two QS-locked mutants (without AphA and HapR) grown with glucose as the sole fermentable sugar. We analyzed the metabolite profiles of the two QS-locked mutants up to 19 h after inoculation to avoid measurement of metabolites that might leak from dead cells (Fig. 3B). By using an unbiased nuclear magnetic resonance (NMR) metabolomic approach (45), more than 20 extracellular metabolites could be detected and quantified (see Table S2 in the supplemental material). No significant difference between the two QS-locked mutants was detected in the concentrations of the majority of these metabolites at multiple time points (see Table S2). However, the concentrations of organic acids derived from pyruvate (i.e., formate, acetate, and lactate) were significantly higher in LCD SCM than in HCD SCM (Fig. 3C to E; see Table S2). Moreover, extracellular levels of the neutral molecules acetoin and 2,3-BD in HCD SCM were significantly higher than those in LCD SCM (Fig. 3F and G; see Table S2). The extracellular metabolome profiles of the WT and a *luxO*$^+$ Δ*aphA* Δ*hapR* mutant were similar to the profiles obtained from the respective isogenic HCD-locked mutants (see Table S2 and Fig. S5 in the supplemental material). Together, these results suggest that *V. cholerae* uses QS, in particular Qrr1-4 sRNAs, to control central carbon metabolism by altering pyruvate flux in favor of organic acid production at LCD and then switching to neutral molecule production at HCD, presumably to regulate the potential overproduction of toxic metabolic by-products. Consistent with our data, the addition of amounts of formic acid, acetic acid, and lactic acid equivalent to those detected in LCD SCM to a culture of the HCD-locked QS mutant was sufficient to kill all of the cells in the population (see Fig. S6 in the supplemental material). In contrast, LCD-locked mutant viability was maintained by buffering the culture medium to a neutral pH (see Fig. S6).

Uncoupling of Qrr1-4 regulation of *alsS* suppresses glucose sensitivity in LCD-locked mutants. We then tested if deletion of the acetoin/2,3-BD biosynthetic operon *alsDSO* (42) from the HCD-locked QS mutant (lacking AphA and HapR) would cause the strain to become sensitive to growth in glucose. Indeed, the *alsDSO* deletion caused the strain to become sensitive to fermen-

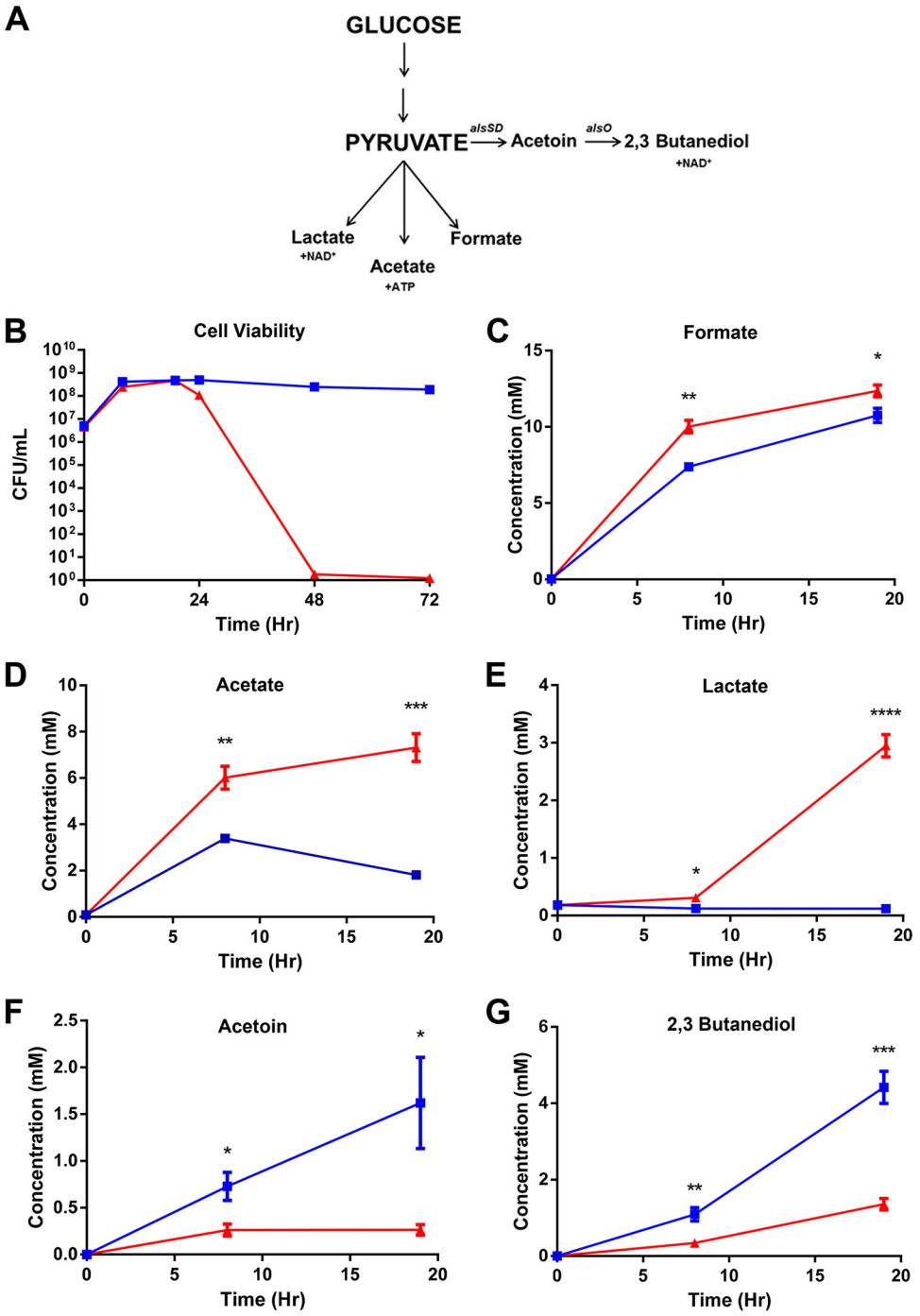

FIG 3 Extracellular metabolite profiles of QS mutants grown under fermentative conditions. (A) Simplified view of glycolysis and pyruvate metabolism in *V. cholerae*. (B) Viability of LCD-locked (*luxO*^{D61E} Δ*aphA* Δ*hapR* Δ*vpsL*; red solid triangles) and HCD-locked (Δ*luxO* Δ*aphA* Δ*hapR* Δ*vpsL*; blue solid squares) cells. Concentrations (millimolar) of formate (C), acetate, (D), lactate (E), acetoin (F), and 2,3-BD (G) in LCD-locked (red solid triangles) and HCD-locked (blue solid squares) mutants. *P* values (Student's *t* test): *, $P < 0.05$; **, $P < 0.01$; ***, $P < 0.001$; ****, $P < 0.0001$. The values shown are averages of at least three replicates. Error bars denote the SEM.

tative stress, similar to the LCD-locked mutant (Fig. 4A). In contrast, overexpression of the *alsDSO* operon under the control of a heterologous promoter and ribosome binding site (RBS) in the LCD-locked mutant (lacking AphA and HapR) relieved glucose sensitivity (Fig. 4B). Strikingly, overexpression of *alsS* alone, but not overexpression of *alsD, alsO*, or *alsR*, encoding the positive transcriptional regulator of the *alsDSO* operon (42), also suppressed the glucose sensitivity of the LCD-locked mutant (Fig. 4B). Overproduction of AlsS alone also caused the extracellular concentrations of acetoin and 2,3-BD to increase in an LCD-locked strain, while acetate and lactate concentrations decreased significantly (Fig. 4C and D). These results are consistent with a

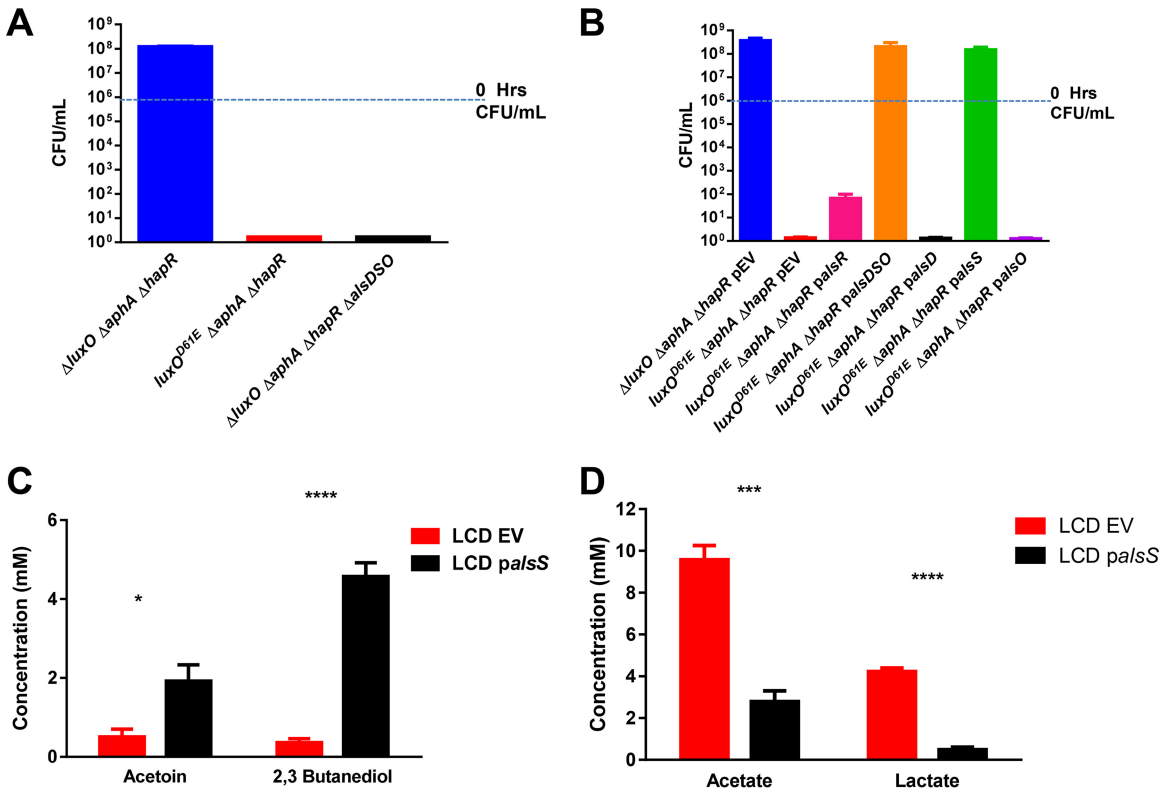

FIG 4 AlsS misregulation causes fermentation stress in QS mutants. (A) Cell viability of the HCD-locked strain (Δ*luxO* Δ*aphA* Δ*hapR* Δ*vpsL*; blue bar), the LCD-locked strain (*luxO*^{D61E} Δ*aphA* Δ*hapR* Δ*vpsL*; red bar), and the HCD-locked strain carrying the Δ*alsDSO* deletion (black bar) at 72 h of growth under fermentative conditions. (B) Cell viability at 72 h of the HCD-locked strain (blue bar), the LCD-locked strain (red bar), and the LCD-locked strain harboring the *als* overexpression plasmids p*alsR* (pink bar), p*alsDSO* (orange bar), p*alsD* (black bar), p*alsS* (green bar), and p*alsO* (purple bar). (C and D) Extracellular concentrations of selected metabolites of the LCD-locked strain (red bars) and the LCD-locked strain with p*alsS* (black bars) grown under fermentative conditions. Millimolar concentrations are shown, and samples were taken at 19 h of growth. The values shown are averages of at least three replicates. Error bars denote the SEM. *P* values (Student's *t* test): *, $P < 0.05$; ***, $P < 0.001$; ****, $P < 0.0001$. EV, empty vector.

model in which production of Qrr1-4 in LCD-locked QS mutants reduces *alsS* expression, leading to sensitivity to fermentative stress.

Qrr sRNAs regulate *alsS* expression post-transcriptionally. To determine the mechanism by which Qrr1-4 reduces *alsS* expression, we constructed AlsS-GFP translational reporters by fusing an isopropyl-β-D-thiogalactopyranoside (IPTG)-inducible P_{tac} promoter to various lengths of the *alsS* 5′ upstream region plus the *alsS* coding region, followed by the gene encoding an unstable version of green fluorescent protein (GFP) (Fig. 5A). We introduced these constructs into both LCD-locked and HCD-locked QS strains lacking HapR and AphA and measured the GFP fluorescence generated from these reporters per cell. The first construct, S1, which contains 44 bp upstream of the start codon of *alsS* with the predicted RBS (Fig. 5A), produced similar amounts of fluorescence in both QS-locked mutants (Fig. 5B). In contrast, LCD-locked mutants harboring the construct S3.3, which contains an additional 150-bp region that extends into the *alsD* gene (Fig. 5A), produced significantly less fluorescence than the HCD-locked mutants carrying the same constructs (Fig. 5B). Isogenic strains carrying a WT *luxO* allele harboring these constructs produced levels of fluorescence similar to those of the HCD-locked mutants (see Fig. S7 in the supplemental material).

To determine if Qrr1-4 directly interacts with the mRNA of *alsS*, we introduced the S1 and S3.3 reporters into a heterologous *Escherichia coli* host (21) that does not normally have the *V. cholerae* QS circuit or the *alsS* gene. Instead, *V. cholerae qrr4* was produced ectopically from a plasmid by using a rhamnose-inducible promoter. Similar GFP levels were detected in strains carrying the S1 construct, whether Qrr4 was overexpressed or not (Fig. 5C). In contrast, GFP expression in the cultures carrying the S3.3 reporter was significantly reduced when Qrr4 was overproduced (Fig. 5C). Although we could not rule out the possibility that Qrr4 has an impact on an unknown *E. coli* factor that could regulate *alsS* expression, our results suggest that Qrr sRNAs likely repress *alsS* expression through a direct mechanism. We also performed quantitative reverse transcription-PCR to determine the *alsS* and *gfp* transcript levels in different *E. coli* reporter cultures with and without Qrr4 overexpression. The *alsS* and *gfp* transcript levels were comparable in all cultures (data not shown), arguing against a role for Qrr sRNAs in transcriptional termination.

We then made a 5′ truncation of the S3.3 construct (Fig. 5A). The resulting construct, S3.4, is 31 bp shorter than the S3.3 construct. We found that repression of GFP production by Qrr sRNAs was abolished in the S3.4 construct in the LCD-locked *V. cholerae* strain (Fig. 5B; see Fig. S7). This region contains the signature ARN/AAN Hfq binding motif (46), suggesting that Qrr sRNAs require Hfq to repress *alsS* expression. Indeed, an LCD-locked mutant with a Δ*hfq* mutation is not sensitive to fermentative stress. In addition, we used an sRNA binding site prediction pro-

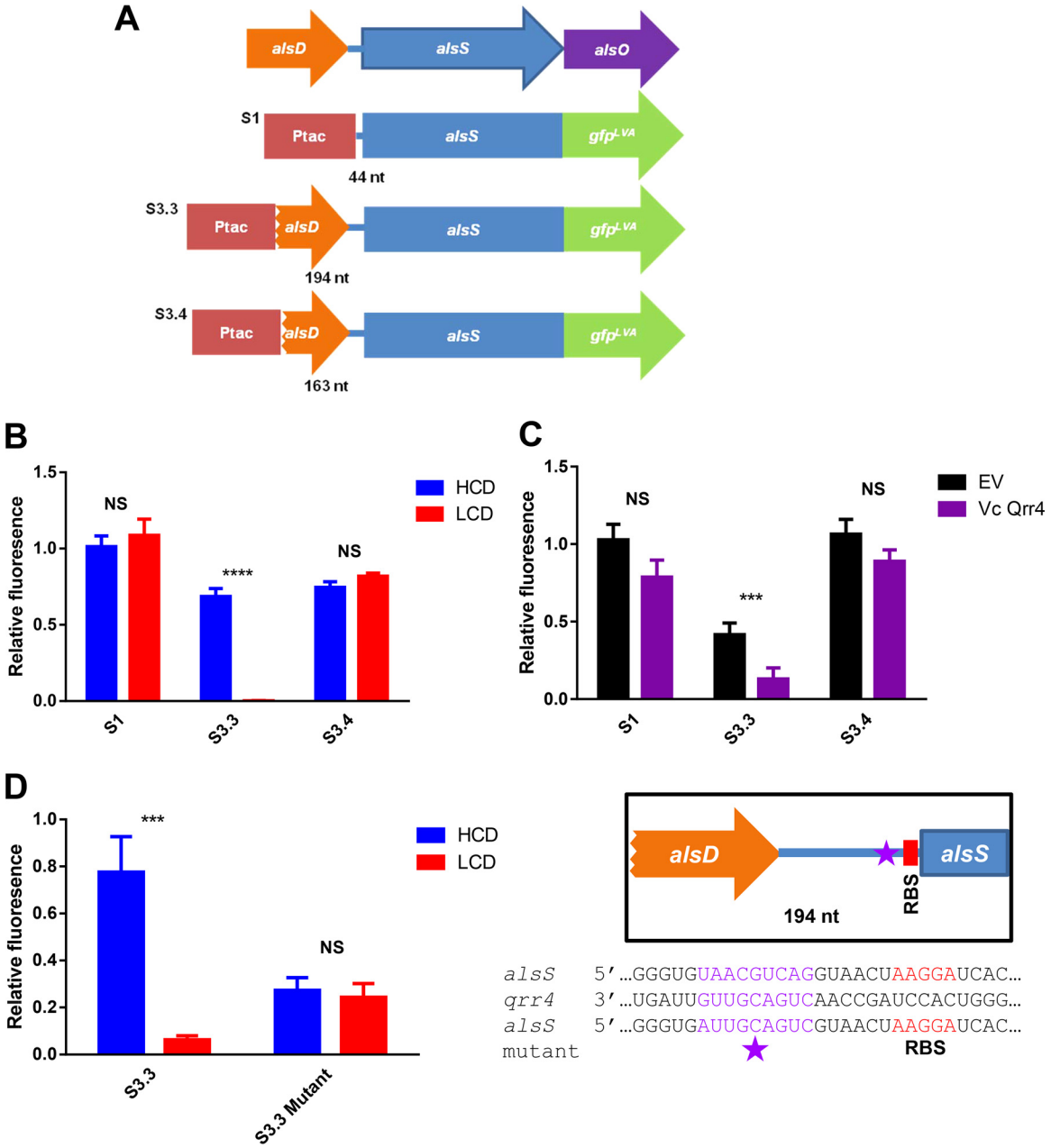

FIG 5 Qrr1-4 regulate *alsS* translation. (A) Depiction of the *alsDSO* operon and the different GFP translational fusions used in this study. nt, nucleotides. (B) Relative GFP fluorescence of different GFP translational fusions in *V. cholerae* HCD-locked (Δ*luxO* Δ*aphA* Δ*hapR* Δ*vpsL*; blue bars) and LCD-locked (*luxO*^{D61E} Δ*aphA* Δ*hapR* Δ*vpsL*; red bars) strains. Each bar is normalized to the median FLU value of the HCD strain harboring the S1 plasmid. (C) Relative GFP fluorescence of different GFP translational fusions in *E. coli* strains either carrying an empty vector (EV) plasmid (black bars) or a plasmid containing rhamnose-induced *V. cholerae qrr4* (purple bars). Each bar is normalized to the median FLU value of the *E. coli* strain carrying the S1 and EV plasmids. (D) Relative GFP fluorescence of GFP translational fusion S3.3 and S3.3 harboring nine consecutive mutations in a predicted Qrr binding site in HCD-locked (blue bars) and LCD-locked (red bars) *V. cholerae* strains. Each bar is normalized to the median FLU value of the HCD strain harboring the S1 plasmid. Highlighted are the location of a hypothetical Qrr binding site in *alsS* (purple star), the sequence of the mutant construct, and the predicted RBS. The values shown are averages of at least three replicates. Error bars denote the SEM. *P* values (Student's *t* test): ***, $P < 0.001$; ****, $P < 0.0001$. NS, no statistical significance.

gram, IntaRNA (47, 48), to locate a potential Qrr binding site within the *alsS* 5′ untranslated region (UTR). The program predicted a consecutive nine-nucleotide putative Qrr binding site just six nucleotides 5′ to the predicted RBS of *alsS* (Fig. 5D). Mutation of this site in the S3.3 construct lowered the overall GFP production level but abolished the repression by Qrr sRNAs in the *V. cholerae* LCD-locked strain (Fig. 5D), suggesting that Qrr sRNAs could potentially bind to this site and occlude the ribosome from translating the *alsS* transcript. However, when we introduced this mutated construct into the heterologous *E. coli* host, we could not detect any GFP production, regardless of whether Qrr4 was expressed or not. Similarly, mutation of this site in the S3.4

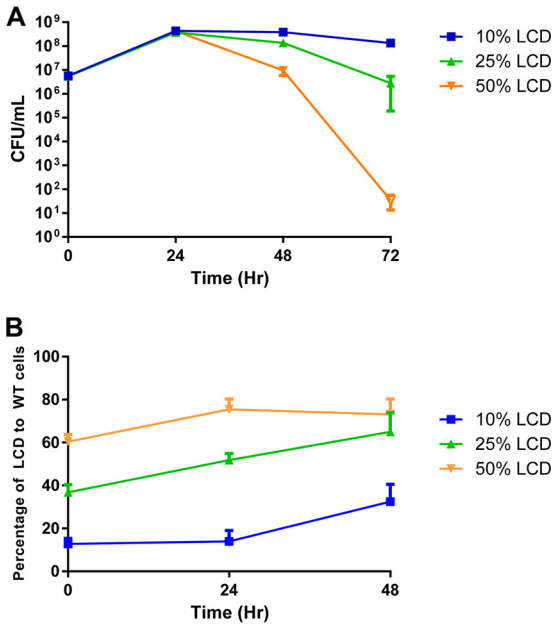

FIG 6 Population stability requires cooperative expression of carbon metabolic genes. (A) Cell viability under fermentative conditions. (B) Percentage of LCD-locked cells present in the overall culture over time. The coculture experiments commenced with different ratios of LCD-locked (*luxO*^{D61E} Δ*vpsL*) QS mutant to WT (Δ*vpsL*) bacteria as shown. The limit of detection at 72 h is 1 cell/ml of culture (open symbol). The values shown are averages of at least three replicates. Error bars denote the SEM.

construct abolished GFP production. The lack of GFP expression in these mutated constructs in *E. coli* could be due to poor recognition of these sequences by the *E. coli* ribosome. Together, our results strongly suggest that Qrr sRNAs repress *alsS* expression through a posttranscriptional mechanism.

Community stability requires coordinated control of pyruvate metabolism. QS is generally assumed to coordinate cooperative behaviors. Why, then, is it used to regulate pyruvate flux and determine the level of expression of acetoin/2,3-BD production? Organic acid production pathways can be viewed as beneficial to individual bacteria because they generate one ATP per pyruvate consumed; however, this process also exploits the common environment that the group inhabits, resulting in acidification of the extracellular milieu. In contrast, the acetoin/2,3-BD production pathway regenerates NAD^+ but does not lower the environmental pH, making it more appropriate for a relatively dense population, and can be considered a "cooperative" behavior in which each individual sacrifices its own fitness to maintain a habitable environment. On the basis of these assumptions, we asked if a cooperative population would form a stable community and if "selfish" individuals have better fitness when present in small numbers but would cause a tragedy of the commons when they become predominant in the population (49–52). We mixed different percentages of LCD-locked mutant (*luxO*^{D61E}) and WT *V. cholerae* cells together and cocultured the two strains in the presence of glucose (Fig. 6A). When the initial percentage of the LCD-locked mutant in the population was ~10%, the entire group remained stable and the total viable cell count after 72 h of growth was similar to that of a population composed entirely of 100% WT cells (Fig. 6A; see Fig. S8A and B in the supplemental material). The percentage of the LCD-locked mutant in this group was maintained at approximately 10% for the first 24 h and increased to ~30% at 48 h, but it did not take over the population (Fig. 6B). The increase in the abundance of LCD-locked mutants in this group suggests that the strain has higher individual fitness than the WT, likely because of an increased ATP yield generated from pyruvate conversion to acetate. In a mixed population containing ~25% LCD-locked mutants and 75% WT bacteria, a slight decrease in the overall population viability was detected at both 48 and 72 h, concurrent with an ~2-fold increase in the percentage of LCD-locked mutants in the population. When 50% of the LCD-locked mutant and 50% of the WT bacteria were cocultured at the outset of the experiment, massive cell death resulting in total population collapse was observed (Fig. 6A). The percentage of LCD-locked mutants in this group increased only slightly (<2-fold), but they represented more than half of the population (Fig. 6B). Rapid killing of the entire population was observed when LCD-locked QS mutants were present at even higher percentages (see Fig. S8A and B). Similar results were obtained when *luxO*^{D61E} mutants were cocultured with Δ*luxO* mutants (see Fig. S8C and D). Together, these results suggest that the choice between organic acid production and acetoin/2,3-BD production has to be coordinated and cooperative in order to maintain long-term population stability, and QS has evolved to minimize the danger to the population by preventing uncontrolled acidification of the shared environment.

DISCUSSION

Here we show that Qrr sRNAs play a unique role in maintaining population stability by coordinating pyruvate metabolism. While QS has been shown to affect carbon metabolism (acetate switch) in other *Vibrio* species (53), we illustrate here a new role for Qrr1-4 in metabolic regulation through coordinating the flux of the key carbon metabolite pyruvate at different cell densities. Our new data suggest that, in addition to AphA, a QS regulator that has been previously shown to repress the transcription of the *alsDSO* operon (42), Qrr1-4 sRNAs ensure that acetoin and 2,3-BD are not produced by blocking *alsS* translation. Furthermore, (p)ppGpp (a product of the stringent response) positively regulates the transcription of the *alsDSO* operon in *V. cholerae* and (p)ppGpp-null mutants lose viability because of fermentative stress (43). Our results and those of others, taken together, suggest that multiple layers of regulation are employed to control acetoin/2,3-BD production in *V. cholerae*. Our new results also expand the repertoire of sRNAs that regulate carbon metabolism in bacteria (54–58).

Acetoin and 2,3-BD production has been shown to be activated by QS in other species besides *V. cholerae* (59, 60), but it is unclear what the evolutionary advantage of employing QS for such regulation is. Although it is generally believed that QS is used to coordinate and modulate cooperative behaviors at the population level, metabolic flux control is not usually perceived as a social behavior. We propose here, however, that organic acid production and neutral metabolite production can be considered two contrasting social traits. Our data suggest that QS allows cells to maximize individual fitness when the cell number in the population is low, as reflected by the increase in the proportion of LCD-locked strains in mixed cultures with WT or HCD-locked strains. At LCD, there is little incentive for cells to make acetoin and 2,3-BD, as ATP is not produced through this pathway. However, continuous production of organic acids could lead to acidification of

the extracellular milieu, and *V. cholerae* is known to have low tolerance for a low pH (61). Thus, *V. cholerae* has evolved to sacrifice the ability to produce ATP via the acetate synthesis pathway and switch pyruvate flux to the production of the neutral molecules acetoin and 2,3-BD to maintain a sustainable and well-preserved environment to prevent population collapse at HCD. Interestingly, although many *V. cholerae* strains carry the *alsDSO* operon, production of acetoin and 2,3-BD is observed mainly in the *V. cholerae* O1 El Tor serotype, the current pandemic strain (44). Metabolic slowing due to QS-dependent nutrient uptake restriction has also been observed in *Burkholderia glumae* (62).

A similar scenario was observed in some *Burkholderia* species in which QS-positive bacteria produce oxalate, an extracellular metabolite that neutralizes the ammonia released during amino acid catabolism (63). Thus, QS in *Burkholderia* is used to anticipate overcrowding and promote bacterial survival, and QS mutants that fail to produce oxalate encounter massive and rapid population crashes (63). However, unlike the study here, oxalate production and amino acid catabolism in *Burkholderia* do not involve common precursor metabolites. Thus, these two pathways likely are not mutually exclusive and it is unclear what the fitness cost is for cooperative QS-positive cells to produce oxalate as a benefit to the group (63).

While QS seems to be an effective mechanism to enable cooperation in a population to cope with metabolic stresses due to increasing cell density, this collective behavior can be exploited by social cheaters, which are noncooperative individuals that take advantage of common goods. In many cases, the common goods are extracellular enzymes (49, 64, 65) or shared chemical molecules (e.g., rhamnolipid surfactant) (66, 67) to which cheaters can gain access without their own contribution. In our case, we consider that the "common goods" are not the extracellular metabolites acetoin and 2,3-BD, since these compounds do not neutralize the organic acids that accumulate during growth. Instead, the shared resource is the extracellular environment that both cheaters and cooperators inhabit. We show that the introduction of large quantities of LCD-locked QS mutants (cheaters) leads to a tragedy of the commons (i.e., rapid deterioration of the shared environment) and causes massive population killing.

While LCD-locked QS mutants have been found in natural settings (12, 68, 69), their occurrence is restricted and could be due to selection during growth in laboratories. Indeed, most of the *V. cholerae* strains recently isolated from patient stool samples appear to be QS positive (70), as determined by their natural transformability, a trait that is strictly dependent on a functional QS system. It is possible that rapid killing by fermentative stress is sufficient to eliminate uncooperative subpopulations (i.e., QS-negative LCD-locked mutants), especially in a structurally complex environment where diffusion is limited (71, 72). Alternatively, bacteria have evolved several mechanisms to curb social cheating, including spatial structuring, policing, metabolic constraint, and metabolic prudence (49, 64–66, 71, 73). *V. cholerae* may have evolved to use one or more of these previously described mechanisms to enforce cooperation within the population, and these sustainable bacteria eventually outcompete those that kill themselves with toxic waste.

MATERIALS AND METHODS

Strains, plasmids, and culture conditions. All of the *V. cholerae* strains used in this study were derived from C6706str2, a streptomycin-resistant isolate of C6706 (O1 El Tor) (74). *E. coli* S17-1 λpir was used as a host for plasmids for mating into *V. cholerae* and for *E. coli* GFP assays. All of the strains used in this study are described in Table S1 in the supplemental material. *V. cholerae* and *E. coli* cultures were grown overnight with aeration in Luria-Bertani (LB) broth at 30°C. Cell viability assays were carried out in static culture at 30°C in 1× M9 medium (25.2 mM Na_2HPO_4, 22 mM KH_2PO_4, 8.56 mM NaCl, 2 mM $MgSO_4$, 0.1 mM $CaCl_2$) with 0.2% Casamino acids. As a carbon source, 0.5% glucose, 0.5% GlcNAc, or 0.5% glycerol was added. When appropriate, the medium was supplemented with streptomycin (100 μg/ml), ampicillin (100 μg/ml), kanamycin (100 μg/ml), and polymyxin B (50 U/ml).

DNA manipulations and mutant construction. All DNA manipulations were performed by using standard procedures as previously described (15). The oligonucleotide sequences used for PCR and sequencing reactions will be provided upon request. Deletions were introduced into the *V. cholerae* genome by allelic exchange by using the suicide vector pKAS32 as previously described (75). Point mutations were introduced by using the QuikChange site-directed mutagenesis kit (Agilent). Open reading frames of genes of interest were PCR amplified with a heterologous RBS and cloned into vector pEVS143 (76) digested with AvrII and BamHI for overexpression. For unstable GFP translational reporters, we first replaced the gene encoding GFP in pEVS143 (76) with an unstable version obtained from pSLS3 (77). Different *alsS* fragments (5′ UTR with the whole *alsS* reading frame without the stop codon) were cloned immediately upstream of the gene encoding unstable GFP without the start codon. Overexpression of *V. cholerae* Qrr4 was achieved by inserting the *qrr4* gene by using Gibson Assembly (NEB) into pRHA109 that contains a rhamnose-inducible P_{rhaB} promoter (78). All mutant strains were confirmed by sequencing.

Cell viability assays. Overnight cultures were diluted 1,000× and inoculated into M9 minimal medium with 0.2% Casamino acids plus the specified carbon source. Assays were carried out statically at 30°C for at least 72 h. Every 24 h, serial dilutions of each sample were plated to determine viability. Limits of detection are indicated in the figure legends.

SCM toxicity. LCD-locked (*luxO*^{D61E} Δ*aphA* Δ*hapR* Δ*vpsL*) and HCD-locked (Δ*luxO* Δ*aphA* Δ*hapR* Δ*vpsL*) QS mutants were grown under fermentative conditions as described above for 72 h. At 72 h, the cells were centrifuged at 3,000 rpm for 15 min. The supernatant was filtered and inoculated with fresh overnight cultures of LCD- and HCD-locked QS mutants diluted 1,000×. Cells were allowed to grow statically at 30°C for 72 h, with an aliquot plated every 24 h to measure cell viability. A universal indicator was used to record the pH at each time point (Fluka Analytical). For assays in which organic acids were added back to determine cell viability, we determined the concentrations of organic acids at 8, 19, 24, 48, and 72 h by NMR metabolomics and added back the total amounts of lactate, acetate, and formate found in LCD SCM at these time points to the HCD culture. For the LCD neutralization experiment, Tris base was added to the SCM until the pH reached 7.2, and then the neutralized SCM was inoculated with fresh LCD cells and cells were plated to determine overall viability at 0, 24, 48, and 72 h.

NMR metabolomics. Extracellular metabolite analysis was done with supernatants taken from the growth of LCD (*luxO*^{D61E} Δ*aphA* Δ*hapR* Δ*vpsL*) and HCD (Δ*luxO* Δ*aphA* Δ*hapR* Δ*vpsL*) QS mutants and an isogenic Δ*aphA* Δ*hapR* Δ*vpsL* mutant strain grown under fermentative conditions as described above. Cells were centrifuged at 3,000 rpm for 15 min. Supernatants were removed from the pellets, sterile filtered through a syringe filter (0.2 μM PES), and stored at −20°C until NMR analysis. Five hundred microliters of the supernatants was transferred to 7-in., 600-MHz NMR tubes (Wilmad). A final concentration of 0.180 mM 4,4-dimethyl-4-silapentane-1-sulfonic acid (DSS) in D_2O was added to every sample as an internal standard. A ^{1}H NMR spectrum of each sample was collected at 25°C on a Bruker Avance 600 spectrometer by using 128 scans and a NOE1D pulse sequence. NMR data were compared to known databases (79), as well as against authentic compounds. The data were processed and analyzed by using CHENOMX (version 8.0) for quantification

(45). Data were also analyzed by using Bayesil (80, 81). The average value and the standard error of the mean (SEM) were determined for at least three replicates.

GFP expression analysis. Fluorescence levels of translational fusions were determined as previously described (21). Overnight cultures were diluted 1,000× and allowed to grow in M9 minimal medium plus 0.2% Casamino acids and 0.5% glycerol to avoid cell killing by glucose fermentation and to uncouple any effect of acetate accumulation. For *V. cholerae* assays, 50 μM IPTG was added to the medium when appropriate. For *E. coli* assays, 50 μM IPTG and/or 1 mM rhamnose was added to the medium when appropriate. The GFP signal was measured at an optical density at 600 nm (OD_{600}) of approximately 0.1 on a BioTek plate reader at 30°C. The number of fluorescence units (FLU) was calculated by dividing the GFP fluorescence signal by the OD_{600}. Fifty microliters of mineral oil was added to each well to prevent evaporation in the plate reader. The average value and the SEM were determined for at least three replicates.

Coculture experiments. Overnight cultures were diluted to matching ODs and then diluted further to 1,000× for the assay. The assays were done in M9 minimal medium plus 0.2% Casamino acids and 0.5% glucose. Different ratios of LCD (*luxO*^{D61E} Δ*vpsL*) and HCD (Δ*luxO* Δ*vpsL* Δ*lacZ*) or WT (Δ*vpsL* Δ*lacZ*) bacteria were mixed and grown statically for 72 h at 30°C. *V. cholerae* population viability was measured by plating serial dilutions at 24-h intervals on LB–streptomycin–5-bromo-4-chloro-3-indolyl-β-D-galactopyranoside (X-Gal) plates to determine end ratios by using blue versus white colonies plus LB plates to determine total population viability. Limits of detection are indicated in the figure legends. The average value and the SEM were determined for at least three replicates.

SUPPLEMENTAL MATERIAL

Supplemental material for this article may be found at http://mbio.asm.org/lookup/suppl/doi:10.1128/mBio.01863-16/-/DCSupplemental.

Figure S1, TIF file, 0.4 MB.
Figure S2, TIF file, 0.2 MB.
Figure S3, TIF file, 0.2 MB.
Figure S4, TIF file, 0.3 MB.
Figure S5, TIF file, 2.1 MB.
Figure S6, TIF file, 0.3 MB.
Figure S7, TIF file, 0.5 MB.
Figure S8, TIF file, 1.1 MB.
Table S1, PDF file, 0.1 MB.
Table S2, PDF file, 0.3 MB.

ACKNOWLEDGMENTS

We thank Joao Xavier and Linc Sonenshein for critical comments on the manuscript. We thank Christine Chapman for her technical contributions and members in the Ng Lab for helpful discussions.

This work was supported by NIH T32 AI007329 (L.A.H.) and the Russo Collaborative Research Fund (W.L.N. and J.B.).

FUNDING INFORMATION

This work, including the efforts of Wai-Leung Ng and James D. Baleja, was funded by Russo Collaborative Research Fund. This work, including the efforts of Lisa A. Hawver, was funded by National Institute of Allergy and Infectious Diseases (NIAID) (T32AI007329).

REFERENCES

1. **Miller MB, Bassler BL.** 2001. Quorum sensing in bacteria. Annu Rev Microbiol **55:**165–199. http://dx.doi.org/10.1146/annurev.micro.55.1.165.
2. **Ng WL, Bassler BL.** 2009. Bacterial quorum-sensing network architectures. Annu Rev Genet **43:**197–222. http://dx.doi.org/10.1146/annurev-genet-102108-134304.
3. **Waters CM, Bassler BL.** 2005. Quorum sensing: cell-to-cell communication in bacteria. Annu Rev Cell Dev Biol **21:**319–346. http://dx.doi.org/10.1146/annurev.cellbio.21.012704.131001.
4. **Novick RP, Geisinger E.** 2008. Quorum sensing in staphylococci. Annu Rev Genet **42:**541–564. http://dx.doi.org/10.1146/annurev.genet.42.110807.091640.
5. **Goo E, An JH, Kang Y, Hwang I.** 2015. Control of bacterial metabolism by quorum sensing. Trends Microbiol **23:**567–576. http://dx.doi.org/10.1016/j.tim.2015.05.007.
6. **Shikuma NJ, Fong JC, Odell LS, Perchuk BS, Laub MT, Yildiz FH.** 2009. Overexpression of VpsS, a hybrid sensor kinase, enhances biofilm formation in *Vibrio cholerae*. J Bacteriol **191:**5147–5158. http://dx.doi.org/10.1128/JB.00401-09.
7. **Antonova ES, Hammer BK.** 2011. Quorum-sensing autoinducer molecules produced by members of a multispecies biofilm promote horizontal gene transfer to *Vibrio cholerae*. FEMS Microbiol Lett **322:**68–76. http://dx.doi.org/10.1111/j.1574-6968.2011.02328.x.
8. **Bardill JP, Hammer BK.** 2012. Non-coding sRNAs regulate virulence in the bacterial pathogen *Vibrio cholerae*. RNA Biol **9:**392–401. http://dx.doi.org/10.4161/rna.19975.
9. **Hammer BK, Bassler BL.** 2003. Quorum sensing controls biofilm formation in *Vibrio cholerae*. Mol Microbiol **50:**101–104. http://dx.doi.org/10.1046/j.1365-2958.2003.03688.x.
10. **Zhu J, Mekalanos JJ.** 2003. Quorum sensing-dependent biofilms enhance colonization in *Vibrio cholerae*. Dev Cell **5:**647–656. http://dx.doi.org/10.1016/S1534-5807(03)00295-8.
11. **Zhu J, Miller MB, Vance RE, Dziejman M, Bassler BL, Mekalanos JJ.** 2002. Quorum-sensing regulators control virulence gene expression in *Vibrio cholerae*. Proc Natl Acad Sci U S A **99:**3129–3134. http://dx.doi.org/10.1073/pnas.052694299.
12. **Blokesch M.** 2012. A quorum sensing-mediated switch contributes to natural transformation of *Vibrio cholerae*. Mob Genet Elements **2:**224–227. http://dx.doi.org/10.4161/mge.22284.
13. **Lo Scrudato M, Blokesch M.** 2012. The regulatory network of natural competence and transformation of *Vibrio cholerae*. PLoS Genet **8:**e1002778. http://dx.doi.org/10.1371/journal.pgen.1002778.
14. **Suckow G, Seitz P, Blokesch M.** 2011. Quorum sensing contributes to natural transformation of *Vibrio cholerae* in a species-specific manner. J Bacteriol **193:**4914–4924. http://dx.doi.org/10.1128/JB.05396-11.
15. **Jung SA, Chapman CA, Ng WL.** 2015. Quadruple quorum-sensing inputs control *Vibrio cholerae* virulence and maintain system robustness. PLoS Pathog **11:**e1004837. http://dx.doi.org/10.1371/journal.ppat.1004837.
16. **Bardill JP, Zhao X, Hammer BK.** 2011. The *Vibrio cholerae* quorum sensing response is mediated by Hfq-dependent sRNA/mRNA base pairing interactions. Mol Microbiol **80:**1381–1394. http://dx.doi.org/10.1111/j.1365-2958.2011.07655.x.
17. **Hammer BK, Bassler BL.** 2007. Regulatory small RNAs circumvent the conventional quorum sensing pathway in pandemic *Vibrio cholerae*. Proc Natl Acad Sci U S A **104:**11145–11149. http://dx.doi.org/10.1073/pnas.0703860104.
18. **Lenz DH, Mok KC, Lilley BN, Kulkarni RV, Wingreen NS, Bassler BL.** 2004. The small RNA chaperone Hfq and multiple small RNAs control quorum sensing in *Vibrio harveyi* and *Vibrio cholerae*. Cell **118:**69–82. http://dx.doi.org/10.1016/j.cell.2004.06.009.
19. **Shao Y, Bassler BL.** 2012. Quorum-sensing non-coding small RNAs use unique pairing regions to differentially control mRNA targets. Mol Microbiol **83:**599–611. http://dx.doi.org/10.1111/j.1365-2958.2011.07959.x.
20. **Miller MB, Skorupski K, Lenz DH, Taylor RK, Bassler BL.** 2002. Parallel quorum sensing systems converge to regulate virulence in *Vibrio cholerae*. Cell **110:**303–314. http://dx.doi.org/10.1016/S0092-8674(02)00829-2.
21. **Rutherford ST, van Kessel JC, Shao Y, Bassler BL.** 2011. AphA and LuxR/HapR reciprocally control quorum sensing in vibrios. Genes Dev **25:**397–408. http://dx.doi.org/10.1101/gad.2015011.
22. **Feng L, Rutherford ST, Papenfort K, Bagert JD, van Kessel JC, Tirrell DA, Wingreen NS, Bassler BL.** 2015. A qrr noncoding RNA deploys four different regulatory mechanisms to optimize quorum-sensing dynamics. Cell **160:**228–240. http://dx.doi.org/10.1016/j.cell.2014.11.051.
23. **Svenningsen SL, Waters CM, Bassler BL.** 2008. A negative feedback loop involving small RNAs accelerates *Vibrio cholerae*'s transition out of quorum-sensing mode. Genes Dev **22:**226–238. http://dx.doi.org/10.1101/gad.1629908.
24. **Zhao X, Koestler BJ, Waters CM, Hammer BK.** 2013. Post-transcriptional activation of a diguanylate cyclase by quorum sensing small RNAs promotes biofilm formation in *Vibrio cholerae*. Mol Microbiol **89:**989–1002. http://dx.doi.org/10.1111/mmi.12325.

25. **Shao Y, Bassler BL**. 2014. Quorum regulatory small RNAs repress type VI secretion in *Vibrio cholerae*. Mol Microbiol **92:**921–930. http://dx.doi.org/10.1111/mmi.12599.
26. **Papenfort K, Förstner KU, Cong JP, Sharma CM, Bassler BL**. 2015. Differential RNA-seq of *Vibrio cholerae* identifies the VqmR small RNA as a regulator of biofilm formation. Proc Natl Acad Sci U S A **112:** E766–E775. http://dx.doi.org/10.1073/pnas.1500203112.
27. **Shao Y, Feng L, Rutherford ST, Papenfort K, Bassler BL**. 2013. Functional determinants of the quorum-sensing non-coding RNAs and their roles in target regulation. EMBO J **32:**2158–2171. http://dx.doi.org/10.1038/emboj.2013.155.
28. **Houot L, Chang S, Absalon C, Watnick PI**. 2010. *Vibrio cholerae* phosphoenolpyruvate phosphotransferase system control of carbohydrate transport, biofilm formation, and colonization of the germfree mouse intestine. Infect Immun **78:**1482–1494. http://dx.doi.org/10.1128/IAI.01356-09.
29. **Houot L, Chang S, Pickering BS, Absalon C, Watnick PI**. 2010. The phosphoenolpyruvate phosphotransferase system regulates *Vibrio cholerae* biofilm formation through multiple independent pathways. J Bacteriol **192:**3055–3067. http://dx.doi.org/10.1128/JB.00213-10.
30. **Houot L, Watnick PI**. 2008. A novel role for enzyme I of the *Vibrio cholerae* phosphoenolpyruvate phosphotransferase system in regulation of growth in a biofilm. J Bacteriol **190:**311–320. http://dx.doi.org/10.1128/JB.01410-07.
31. **Pickering BS, Lopilato JE, Smith DR, Watnick PI**. 2014. The transcription factor Mlc promotes *Vibrio cholerae* biofilm formation through repression of phosphotransferase system components. J Bacteriol **196:** 2423–2430. http://dx.doi.org/10.1128/JB.01639-14.
32. **Pickering BS, Smith DR, Watnick PI**. 2012. Glucose-specific enzyme IIA has unique binding partners in the *Vibrio cholerae* biofilm. mBio **3:**e00228-12. http://dx.doi.org/10.1128/mBio.00228-12.
33. **Ymele-Leki P, Houot L, Watnick PI**. 2013. Mannitol and the mannitol-specific enzyme IIB subunit activate *Vibrio cholerae* biofilm formation. Appl Environ Microbiol **79:**4675–4683. http://dx.doi.org/10.1128/AEM.01184-13.
34. **Fong JC, Yildiz FH**. 2008. Interplay between cyclic AMP-cyclic AMP receptor protein and cyclic di-GMP signaling in *Vibrio cholerae* biofilm formation. J Bacteriol **190:**6646–6659. http://dx.doi.org/10.1128/JB.00466-08.
35. **Minato Y, Fassio SR, Wolfe AJ, Häse CC**. 2013. Central metabolism controls transcription of a virulence gene regulator in *Vibrio cholerae*. Microbiology **159:**792–802. http://dx.doi.org/10.1099/mic.0.064865-0.
36. **Oh YT, Lee KM, Bari W, Kim HY, Kim HJ, Yoon SS**. 2016. Cholera toxin production induced upon anaerobic respiration is suppressed by glucose fermentation in *Vibrio cholerae*. J Microbiol Biotechnol **26:** 627–636. http://dx.doi.org/10.4014/jmb.1512.12039.
37. **Liang W, Pascual-Montano A, Silva AJ, Benitez JA**. 2007. The cyclic AMP receptor protein modulates quorum sensing, motility and multiple genes that affect intestinal colonization in *Vibrio cholerae*. Microbiology **153:**2964–2975. http://dx.doi.org/10.1099/mic.0.2007/006668-0.
38. **Silva AJ, Benitez JA**. 2004. Transcriptional regulation of *Vibrio cholerae* hemagglutinin/protease by the cyclic AMP receptor protein and RpoS. J Bacteriol **186:**6374–6382. http://dx.doi.org/10.1128/JB.186.19.6374-6382.2004.
39. **Fong JC, Syed KA, Klose KE, Yildiz FH**. 2010. Role of *Vibrio* polysaccharide (*vps*) genes in VPS production, biofilm formation and *Vibrio cholerae* pathogenesis. Microbiology **156:**2757–2769. http://dx.doi.org/10.1099/mic.0.040196-0.
40. **Yildiz FH, Dolganov NA, Schoolnik GK**. 2001. VpsR, a member of the response regulators of the two-component regulatory systems, is required for expression of *vps* biosynthesis genes and EPS(ETr)-associated phenotypes in *Vibrio cholerae* O1 El Tor. J Bacteriol **183:**1716–1726. http://dx.doi.org/10.1128/JB.183.5.1716-1726.2001.
41. **Zamorano-Sánchez D, Fong JC, Kilic S, Erill I, Yildiz FH**. 2015. Identification and characterization of VpsR and VpsT binding sites in *Vibrio cholerae*. J Bacteriol **197:**1221–1235. http://dx.doi.org/10.1128/JB.02439-14.
42. **Kovacikova G, Lin W, Skorupski K**. 2005. Dual regulation of genes involved in acetoin biosynthesis and motility/biofilm formation by the virulence activator AphA and the acetate-responsive LysR-type regulator AlsR in *Vibrio cholerae*. Mol Microbiol **57:**420–433. http://dx.doi.org/10.1111/j.1365-2958.2005.04700.x.
43. **Oh YT, Lee KM, Bari W, Raskin DM, Yoon SS**. 2015. (p)ppGpp, a small nucleotide regulator, directs the metabolic fate of glucose in *Vibrio cholerae*. J Biol Chem **290:**13178–13190. http://dx.doi.org/10.1074/jbc.M115.640466.
44. **Yoon SS, Mekalanos JJ**. 2006. 2,3-Butanediol synthesis and the emergence of the *Vibrio cholerae* El Tor biotype. Infect Immun **74:**6547–6556. http://dx.doi.org/10.1128/IAI.00695-06.
45. **Weljie AM, Newton J, Mercier P, Carlson E, Slupsky CM**. 2006. Targeted profiling: quantitative analysis of 1H NMR metabolomics data. Anal Chem **78:**4430–4442. http://dx.doi.org/10.1021/ac060209g.
46. **Schu DJ, Zhang AX, Gottesman S, Storz G**. 2015. Alternative Hfq-sRNA interaction modes dictate alternative mRNA recognition. EMBO J **34:** 2557–2573. http://dx.doi.org/10.15252/embj.201591569.
47. **Busch A, Richter AS, Backofen R**. 2008. IntaRNA: efficient prediction of bacterial sRNA targets incorporating target site accessibility and seed regions. Bioinformatics **24:**2849–2856. http://dx.doi.org/10.1093/bioinformatics/btn544.
48. **Wright PR, Georg J, Mann M, Sorescu DA, Richter AS, Lott S, Kleinkauf R, Hess WR, Backofen R**. 2014. CopraRNA and IntaRNA: predicting small RNA targets, networks and interaction domains. Nucleic Acids Res **42:**W119–W123. http://dx.doi.org/10.1093/nar/gku359.
49. **Dandekar AA, Chugani S, Greenberg EP**. 2012. Bacterial quorum sensing and metabolic incentives to cooperate. Science **338:**264–266. http://dx.doi.org/10.1126/science.1227289.
50. **West SA, Griffin AS, Gardner A, Diggle SP**. 2006. Social evolution theory for microorganisms. Nat Rev Microbiol **4:**597–607. http://dx.doi.org/10.1038/nrmicro1461.
51. **Diggle SP, Griffin AS, Campbell GS, West SA**. 2007. Cooperation and conflict in quorum-sensing bacterial populations. Nature **450:**411–414. http://dx.doi.org/10.1038/nature06279.
52. **Rainey PB, Rainey K**. 2003. Evolution of cooperation and conflict in experimental bacterial populations. Nature **425:**72–74. http://dx.doi.org/10.1038/nature01906.
53. **Studer SV, Mandel MJ, Ruby EG**. 2008. AinS quorum sensing regulates the *Vibrio fischeri* acetate switch. J Bacteriol **190:**5915–5923. http://dx.doi.org/10.1128/JB.00148-08.
54. **Papenfort K, Vogel J**. 2014. Small RNA functions in carbon metabolism and virulence of enteric pathogens. Front Cell Infect Microbiol **4:**91. http://dx.doi.org/10.3389/fcimb.2014.00091.
55. **Sonnleitner E, Haas D**. 2011. Small RNAs as regulators of primary and secondary metabolism in *Pseudomonas* species. Appl Microbiol Biotechnol **91:**63–79. http://dx.doi.org/10.1007/s00253-011-3332-1.
56. **Bobrovskyy M, Vanderpool CK**. 2016. Diverse mechanisms of post-transcriptional repression by the small RNA regulator of glucose-phosphate stress. Mol Microbiol **99:**254–273. http://dx.doi.org/10.1111/mmi.13230.
57. **Bobrovskyy M, Vanderpool CK**. 2014. The small RNA SgrS: roles in metabolism and pathogenesis of enteric bacteria. Front Cell Infect Microbiol **4:**61. http://dx.doi.org/10.3389/fcimb.2014.00061.
58. **Vanderpool CK, Gottesman S**. 2004. Involvement of a novel transcriptional activator and small RNA in post-transcriptional regulation of the glucose phosphoenolpyruvate phosphotransferase system. Mol Microbiol **54:**1076–1089. http://dx.doi.org/10.1111/j.1365-2958.2004.04348.x.
59. **Van Houdt R, Aertsen A, Michiels CW**. 2007. Quorum-sensing-dependent switch to butanediol fermentation prevents lethal medium acidification in Aeromonas hydrophila AH-1N. Res Microbiol **158:** 379–385. http://dx.doi.org/10.1016/j.resmic.2006.11.015.
60. **Moons P, Van Houdt R, Vivijs B, Michiels CW, Aertsen A**. 2011. Integrated regulation of acetoin fermentation by quorum sensing and pH in *Serratia plymuthica* RVH1. Appl Environ Microbiol **77:**3422–3427. http://dx.doi.org/10.1128/AEM.02763-10.
61. **Merrell DS, Camilli A**. 1999. The *cadA* gene of *Vibrio cholerae* is induced during infection and plays a role in acid tolerance. Mol Microbiol **34:** 836–849. http://dx.doi.org/10.1046/j.1365-2958.1999.01650.x.
62. **An JH, Goo E, Kim H, Seo YS, Hwang I**. 2014. Bacterial quorum sensing and metabolic slowing in a cooperative population. Proc Natl Acad Sci U S A **111:**14912–14917. http://dx.doi.org/10.1073/pnas.1412431111.
63. **Goo E, Majerczyk CD, An JH, Chandler JR, Seo YS, Ham H, Lim JY, Kim H, Lee B, Jang MS, Greenberg EP, Hwang I**. 2012. Bacterial quorum sensing, cooperativity, and anticipation of stationary-phase stress. Proc Natl Acad Sci U S A **109:**19775–19780. http://dx.doi.org/10.1073/pnas.1218092109.
64. **Katzianer DS, Wang H, Carey RM, Zhu J**. 2015. "Quorum non-sensing":

social cheating and deception in *Vibrio cholerae*. Appl Environ Microbiol **81:**3856–3862. http://dx.doi.org/10.1128/AEM.00586-15.

65. **Wang M, Schaefer AL, Dandekar AA, Greenberg EP**. 2015. Quorum sensing and policing of *Pseudomonas aeruginosa* social cheaters. Proc Natl Acad Sci U S A **112:**2187–2191. http://dx.doi.org/10.1073/pnas.1500704112.
66. **Xavier JB, Kim W, Foster KR**. 2011. A molecular mechanism that stabilizes cooperative secretions in *Pseudomonas aeruginosa*. Mol Microbiol **79:**166–179. http://dx.doi.org/10.1111/j.1365-2958.2010.07436.x.
67. **Boyle KE, Monaco H, van Ditmarsch D, Deforet M, Xavier JB**. 2015. Integration of metabolic and quorum sensing signals governing the decision to cooperate in a bacterial social trait. PLoS Comput Biol **11:** e1004279. http://dx.doi.org/10.1371/journal.pcbi.1004279.
68. **Joelsson A, Liu Z, Zhu J**. 2006. Genetic and phenotypic diversity of quorum-sensing systems in clinical and environmental isolates of *Vibrio cholerae*. Infect Immun **74:**1141–1147. http://dx.doi.org/10.1128/IAI.74.2.1141-1147.2006.
69. **Wang Y, Wang H, Cui Z, Chen H, Zhong Z, Kan B, Zhu J**. 2011. The prevalence of functional quorum-sensing systems in recently emerged *Vibrio cholerae* toxigenic strains. Environ Microbiol Rep **3:**218–222. http://dx.doi.org/10.1111/j.1758-2229.2010.00212.x.
70. **Dalia AB, Seed KD, Calderwood SB, Camilli A**. 2015. A globally distributed mobile genetic element inhibits natural transformation of *Vibrio cholerae*. Proc Natl Acad Sci U S A **112:**10485–10490. http://dx.doi.org/10.1073/pnas.1509097112.
71. **Drescher K, Nadell CD, Stone HA, Wingreen NS, Bassler BL**. 2014. Solutions to the public goods dilemma in bacterial biofilms. Curr Biol **24:**50–55. http://dx.doi.org/10.1016/j.cub.2013.10.030.
72. **Nadell CD, Foster KR, Xavier JB**. 2010. Emergence of spatial structure in cell groups and the evolution of cooperation. PLoS Comput Biol **6:**e1000716. http://dx.doi.org/10.1371/journal.pcbi.1000716.
73. **Bruger E, Waters C**. 2015. Sharing the sandbox: evolutionary mechanisms that maintain bacterial cooperation. F1000Res **4:** Faculty Rev-1504. http://dx.doi.org/10.12688/f1000research.7363.1.
74. **Thelin KH, Taylor RK**. 1996. Toxin-coregulated pilus, but not mannose-sensitive hemagglutinin, is required for colonization by *Vibrio cholerae* O1 El Tor biotype and O139 strains. Infect Immun **64:**2853–2856.
75. **Skorupski K, Taylor RK**. 1996. Positive selection vectors for allelic exchange. Gene **169:**47–52. http://dx.doi.org/10.1016/0378-1119(95)00793-8.
76. **Dunn AK, Millikan DS, Adin DM, Bose JL, Stabb EV**. 2006. New *rfp*- and pES213-derived tools for analyzing symbiotic *Vibrio fischeri* reveal patterns of infection and *lux* expression in situ. Appl Environ Microbiol **72:**802–810. http://dx.doi.org/10.1128/AEM.72.1.802-810.2006.
77. **Tu KC, Bassler BL**. 2007. Multiple small RNAs act additively to integrate sensory information and control quorum sensing in *Vibrio harveyi*. Genes Dev **21:**221–233. http://dx.doi.org/10.1101/gad.1502407.
78. **Giacalone MJ, Gentile AM, Lovitt BT, Berkley NL, Gunderson CW, Surber MW**. 2006. Toxic protein expression in *Escherichia coli* using a rhamnose-based tightly regulated and tunable promoter system. Biotechniques **40:**355–364. http://dx.doi.org/10.2144/000112112.
79. **Wishart DS, Knox C, Guo AC, Eisner R, Young N, Gautam B, Hau DD, Psychogios N, Dong E, Bouatra S, Mandal R, Sinelnikov I, Xia J, Jia L, Cruz JA, Lim E, Sobsey CA, Shrivastava S, Huang P, Liu P, Fang L, Peng J, Fradette R, Cheng D, Tzur D, Clements M, Lewis A, De Souza A, Zuniga A, Dawe M, Xiong Y, Clive D, Greiner R, Nazyrova A, Shaykhutdinov R, Li L, Vogel HJ, Forsythe I**. 2009. HMDB: a knowledgebase for the human metabolome. Nucleic Acids Res **37:**D603–D610. http://dx.doi.org/10.1093/nar/gkn810.
80. **Ravanbakhsh S, Liu P, Bjorndahl TC, Mandal R, Grant JR, Wilson M, Eisner R, Sinelnikov I, Hu X, Luchinat C, Greiner R, Wishart DS**. 2015. Correction: accurate, fully-automated NMR spectral profiling for metabolomics. PLoS One **10:**e0132873. http://dx.doi.org/10.1371/journal.pone.0132873.
81. **Ravanbakhsh S, Liu P, Bjorndahl TC, Bjordahl TC, Mandal R, Grant JR, Wilson M, Eisner R, Sinelnikov I, Hu X, Luchinat C, Greiner R, Wishart DS**. 2015. Accurate, fully-automated NMR spectral profiling for metabolomics. PLoS One **10:**e0124219. http://dx.doi.org/10.1371/journal.pone.0124219.